Proceedings of the ASME 2017 Dynamic Systems and Control Conference
DSCC2017
October 11-13, 2017, Tysons, Virginia, USA

DSCC2017-5046

OPTIMIZATION AND DESIGN PRINCIPLES OF A MINIMAL-WEIGHT, WEARABLE HYDRAULIC POWER SUPPLY

Jonathan D. Nath
University of Minnesota
Minneapolis, MN, USA
nathx037@umn.edu

William K. Durfee
University of Minnesota
Minneapolis, MN, USA
wkdurfee@umn.edu

ABSTRACT

The field of wearable hydraulics for human-assistive devices is expanding. One of the major challenges facing development of these systems is creating lightweight, portable power units. This project's goal was to develop design strategies and guidelines with the use of analytical modeling to minimize the weight of portable hydraulic power supplies in the range of 50-300 W. Steady-state, analytical models were developed and validated for a system containing a lithium-polymer battery, brushless DC motor, and axial-piston pump. Component parameters such as motor size, pump size, and swashplate angle were varied to explore and develop four main design guidelines that can be used by designers to minimize overall system weight. First, it is often not beneficial to select the smallest sized electric motor that can provide the required torque and speed. Second, cooling systems generally do not help reduce overall system weight. Third, the gearbox between the electric motor and pump should be eliminated to reduce system weight. Fourth, iterative modeling is necessary to determine the various range of particular component parameters necessary to result in a minimal-weight system. The analytical model developed takes inputs of desired flowrate, pressure, and runtime, and outputs the combination of pump size, swashplate angle, and motor size that results in a minimal-weight system. The four design principles and the computer simulation are tools that can be used to either design a fully custom, weight-optimized power supply or to aid in the selection of commercially available components for a low-weight power supply.

INTRODUCTION

The goal of this project was to develop design guidelines and optimization techniques for creating minimal-weight, wearable electro-hydraulic power supplies.

Hydraulic actuation systems have several advantages that make them suitable for wearable human-assistive devices. Hydraulics have force and power densities that are an order of magnitude higher than electric machines [1-3]. This allows for the relatively heavy electro-hydraulic power supply to be worn on the users back or waist, while the lightweight actuators can easily be located remotely using hoses to route the high-pressure fluid. Another benefit of hydraulic systems is that they are shown to have very high precision control, especially when compared to pneumatic or electric systems [4].

There are several examples of exoskeletons that utilize the benefits of hydraulic power including Raytheon Sarcos's XOS2 and Lockheed Martin's Human Universal Load Carrier [5]. The most critical factor for maintaining the evolution of devices such as exoskeletons used military applications will be the development of the power supply system [6]. Many current applications require either tethered power systems or noisy power supplies that use internal combustion engines. This project will focus on creating untethered, energy-dense systems that are also quiet and capable of being used in environments such as a hospital or indoor workplace. While minimizing the weight of the power supply is important for all human-assistive devices, it is especially crucial for devices such as an ankle-foot orthosis or a powered arm device, since the weight of the power supply is not supported by the actual device itself, as with full-body exoskeletons.

Previous work in our lab resulted in an untethered power supply for the hydraulic ankle-foot orthosis shown in Figure 1 [7]. The portable power supply is worn on the user's lower back

and the hydraulic actuators, located on the ankle, provide up to 90 Nm of torque to the ankle.

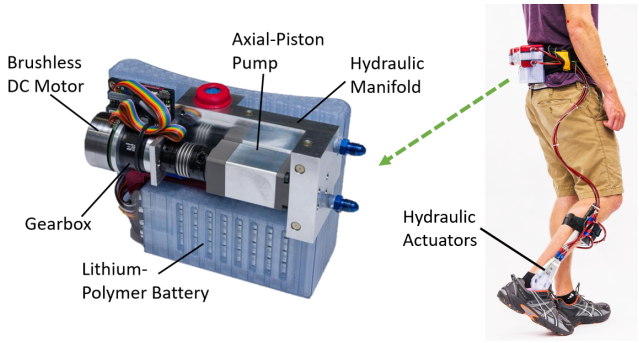

Figure 1. First generation power supply for ankle-foot orthosis

The total weight of this 70 W power supply was 2.2 kg and it could provide up to 12 MPa of pressure. The design of this power supply began with the definition of the maximum required pressure and flowrate. Based off of these requirements, the smallest capable pump was selected. Then, the smallest size of electric motor that could meet the torque and speed requirements was chosen. Finally, a battery was selected that would be able to power the system for the approximate number of desired steps.

After closer analysis, the initial approach used to design this first-generation hydraulic power supply did not prove to be the most effective strategy for creating a minimal-weight system. The reason is that the battery weight needs to be considered, which is impacted by the motor and pump efficiencies. There are cases where heavier electric motors will operate more efficiently than lighter motors. Although the heavier motor adds more initial weight to the system, because it performs more efficiently, this results in a lower battery weight, which may ultimately result in a lower overall system weight. Therefore, in order to explore design principles such as this, analytical models of the power supply components were created to optimize component selection to minimize weight.

METHODS

Model Development

The configuration of the power supply consists of a lithium-polymer battery that supplies power to a brushless DC motor, which then drives an axial-piston pump (Figure 2).

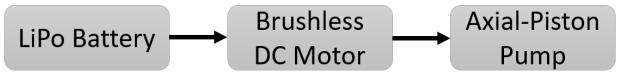

Figure 2. Power supply configuration

Motor Model: Brushless DC motors have several advantages over brushed motors including higher efficiencies, better heat transfer properties, and generally higher power densities [8]. Also, internal combustion engines are not feasible for the desired applications, as these systems are likely to be used indoors, where maintaining low noise levels is a priority.

Motor model parameters such as winding volume, magnet type and size, stator thickness, and rotor parameters were designed using approximate dimensions like that of commercially available DC motors. Motor performance parameters were derived based on this basic motor geometry. For example, the torque characteristic of the motor was determined directly using basic Lorentz force, magnetic field strength, resistivity, and friction equations, as well as simple geometry calculations. Primary losses in the motor include winding losses due to the resistance of the copper winding, mechanical losses such as bearing friction, and iron losses due to such phenomena as eddy currents [9]. The motor model incorporates these losses. Also, the model was designed to scale proportionally, allowing for a wide range of motor power sizes to be explored.

One of the main limiting factors of an electric motor's maximum continuous power output is ensuring that overheating of the windings does not occur. Therefore, a basic heat transfer model was developed shown in Figure 3.

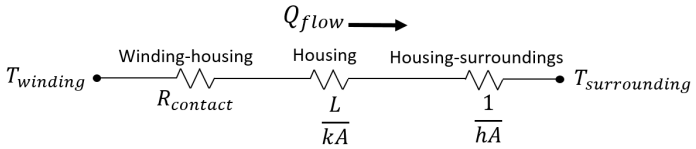

Figure 3. Electric motor heat transfer model

Pump Model: Piston pumps have the highest efficiency among all pump types [10]. Axial-piston pumps also retain relatively high efficiencies at low speeds when compared to other pumps such as gear pumps. Therefore, an axial-piston pump was chosen for this power supply, leaving the modeling of gear pumps and other style pumps for future work.

The axial-piston pump model was adapted from an existing model developed by H. Jeong [11]. This model was modified from its original state to more closely model miniature axial-piston pumps, such as the Takako 0.4 cc/rev and Oildyne 0.17 cc/rev axial-piston pumps, which have simpler features compared to larger-scale pumps.

As with the electric motor model, the pump model was designed to be able to scale proportionally. In addition to overall size, individual component parameters such as the swashplate angle and piston dimensions could easily be varied.

Battery Model: Lithium-polymer batteries were selected due to their relatively high energy density among common battery types. The modeling for the battery was done by obtaining the average energy density for a wide range of commercially available products, which was found to be about 148 Wh/kg [12].

Model Validation

After the analytical models were developed for each power supply component, each model's performance was compared to commercially available products for validation.

Motor Model Validation: The brushless DC motor model was validated by comparing its performance to commercially available motors (Maxon and Micromo Motors). A motor's power rating is the maximum power that a motor can operate at continuously without overheating, as shown by Figure 4 right. Figure 4 left shows the peak efficiency for a range of motor sizes compared to commercially available motors.

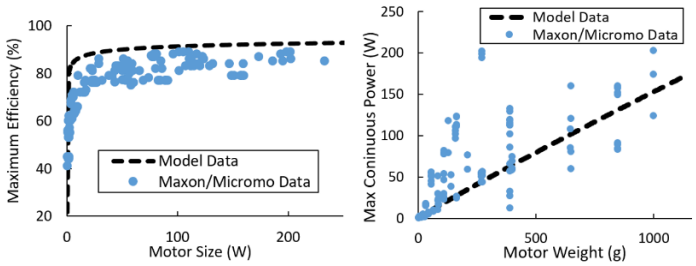

Figure 4. Motor model validation

The motor model adequately fits the commercial data considering that specifications such as the maximum continuous power rating is a parameter that relies heavily on variable aspects such as the particular heat transfer environment that the motor is operating in.

Pump Model Validation: The pump model was validated by comparing it to performance data of the Takako miniature axial-piston pumps. Figure 5 shows the mechanical and volumetric efficiencies for the 0.4 cc/rev pump driven at a constant 200 rad/sec speed and varying pressures.

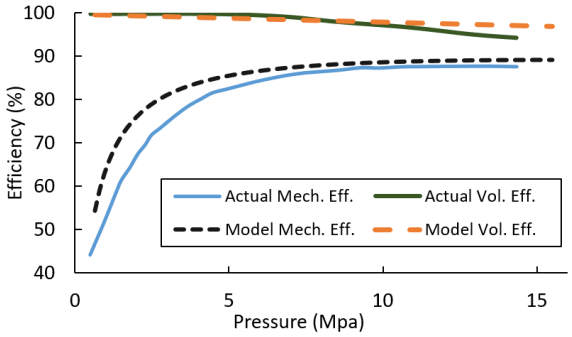

Figure 5. Axial-piston pump validation

Several sizes of the Takako axial-piston pumps, including the 0.8 cc/rev and 1.6 cc/rev, were compared to the pump model, and similar matches in performance efficiencies were observed, thus showing that the model is valid. It has been shown that the energy density and efficiency of hydraulics tend to increase at high pressures [13,14]. Therefore, most of the analyses performed using this model were for pressures exceeding 5 MPa since it is assumed that that the potential applications would utilize higher pressures, such as with the ankle-foot orthosis, which required a maximum of 12 MPa.

After each component model was validated, a combined system model was created. This combined model was used to explore a range of component parameters to aid in the development of design guidelines and principles related to the overall design of a portable hydraulic power supply.

RESULTS

Motor Sizing

To minimize system weight it is not necessarily beneficial to select the smallest motor that can provide the required torque and speed for an application. A case study was done using the verified motor model, where three similar commercially available motors (Maxon EC-i, 70-180 W) were compared at several steady-state operating points. The total system mass, including the motor and battery were compared for the system running at constant 200 rad/sec, 2 hour runtime, and various torques (Figure 6).

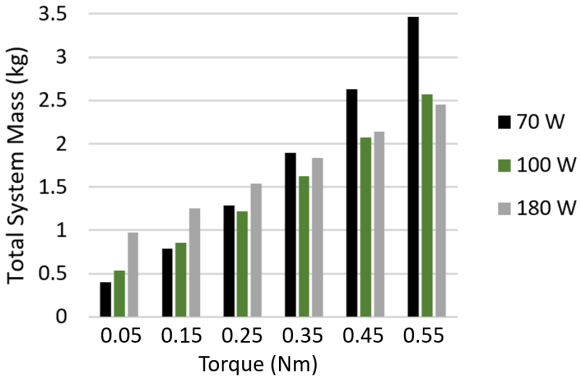

Figure 6. Motor + battery total mass for various steady-state torque conditions

The lighter 70 W motor results in the lowest system weight at the low torque conditions. However, at the higher torque conditions, it is the heavier 180 W motor that produces the lowest system weight. This is because at the higher torque conditions, the larger motor operates more efficiently. Therefore, although the larger motor adds more weight on its own, the higher operating efficiency results in a lower battery weight, and thus a lower overall system weight. This trend is demonstrated in the Figure 7 plot, produced by the validated motor model, with steady-state operation at 100 rad/sec and various steady-state torques.

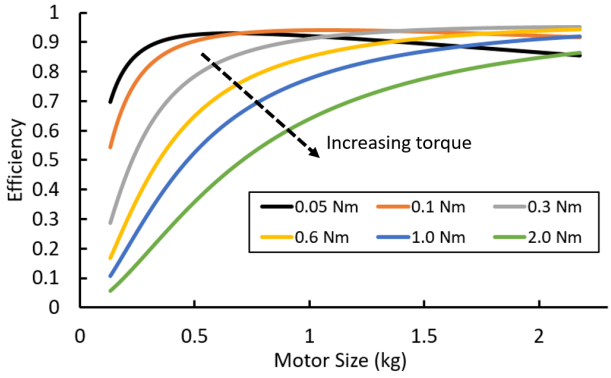

Figure 7. Electric motor efficiency

The reason for this trend of larger motors operating more efficiently, particularly at higher torques, is because the majority of losses come from winding losses [15]. This can be explained by examining the basic equations that govern torque production in an electric motor,

$$T = k_t * I \qquad (1)$$

where the torque produced by the motor, T, is proportional to the current supplied, I. The next equation is the Lorentz force,

$$F = IL\ x\ B \qquad (2)$$

where the force acting on the rotor, F, is proportional to the current supplied times the length of wire windings, L, crossed with the magnetic field strength, B. The equation for resistivity of the windings in the motor is,

$$R = \frac{\rho L}{A} \qquad (3)$$

The winding resistance, R, is proportional to the length of wire divided by the area of the wire cross section, A. Finally, the equation for losses due to winding resistance is,

$$P_w = I^2 R \qquad (4)$$

To see how these equations demonstrate the described trend, assume that there are two motors, one smaller with winding length L, and one larger motor with winding length 2L. Both have equivalent wire diameters and identical magnetic field strength B. To produce an equivalent force with both motors, from equation (2), the larger motor will need half the current since it has twice the length of wire. From equation (3), the resistance of the winding for the larger motor will be twice that of the smaller. Then, using equation (4) for the larger motor, the power loss will be half of the smaller motor. Although the resistance is twice that of the smaller motor, the current is half that of the smaller motor, thus resulting in half the power loss. Although this analysis is simplified, it demonstrates why larger motors operate more efficiently, especially at higher torque conditions.

Another factor that influences motor selection is the desired runtime of the power supply, which is defined by the amount of time the battery would last. Figure 8 shows the results from a case study where a fixed pump size was used and the model was iterated to find what motor size would produce the lowest system weight. A fixed 0.17 cc/rev pump was used and operation conditions of 5 MPa and 5 cc/sec were defined for both plots.

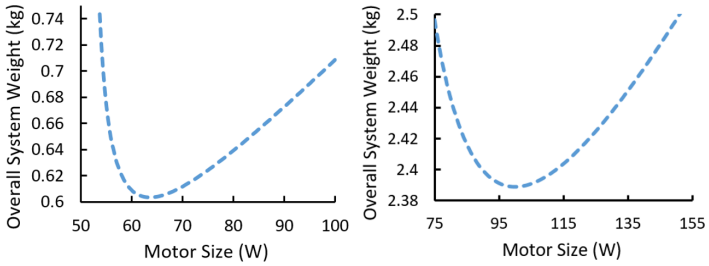

Figure 8. Motor selection, 0.5 hr. runtime (left), 8 hr. runtime (right)

Figure 8 shows how there is one optimal motor size that produces a minimal system weight. A key principle demonstrated by the plots is how the motor size for a minimal-weight system is affected by the desired system runtime, with all other design requirements the same. The motor size that results in a minimal system weight for the 0.5 hour case is around 62 W, while it is 100 W for the 8 hour runtime case. This is because as the desired runtime of the system becomes longer, the weight of the battery dominates the overall system weight. Thus, the operating efficiency of the motor becomes more important than the weight of the motor itself.

These case studies demonstrated that it is often best to select a slightly oversized motor since larger motors often operate more efficiently, which reduces battery weight and therefore overall system weight. Also, selecting larger motors helps to ensure that overheating will not occur in the case of unforeseen heating conditions in real world applications.

Gearbox Elimination

The speed and torque characteristics of electric motors tend to be mismatched from that of pumps. Electric motors generally operate at higher speeds and lower torques than pumps. Two options to correct for this mismatch are to add an often heavy gearbox or to modify the pump characteristics to create lower displacements per revolution. The displacement of an axial-piston pump can be reduced by simply making the overall pump smaller. Also, the swashplate angle can be reduced to lower the displacement. The swashplate angle is easy to modify, and was chosen as the means to modify the torque characteristics of the pump. The torque required to operate a pump is,

$$T_p = \frac{P * A_p * R_p * \tan\alpha * z}{\pi} \qquad (5)$$

where A_P is piston area, R_P is radial pitch, and z is number of pistons. This equation shows that for a given pressure P, the torque required to drive the pump is proportional to the swashplate angle α. The displacement per revolution of the pump also depends on the swashplate angle.

$$V_p = \frac{A_p * R_p * \tan\alpha * \pi}{\sin(\frac{\pi}{2z})} \qquad (6)$$

Equation (6) shows that the displacement per revolution also increases as swashplate angle increases. Therefore, the swashplate angle can be decreased to better match the speed-torque characteristics of the motor. Decreasing the swashplate angle will decrease the displacement per revolution of the pump thus reducing the torque required to produce a desired pressure. Figure 9 shows the effect on efficiency of operating a small pump at steady-state conditions at various fixed swashplate angles. The pump model was used with input dimensions similar to that of the Oildyne 0.17 cc/rev cartridge-piston pump (CP500), with 3 pistons, 7 mm in diameter.

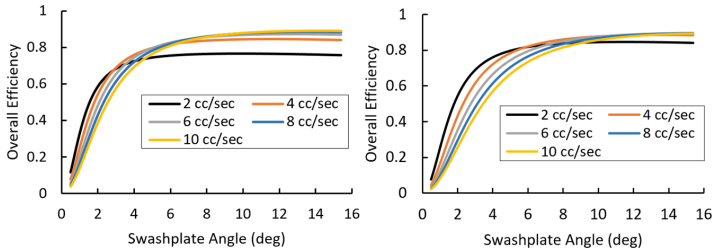

Figure 9. Pump efficiency at 14 MPa (left) and 7 MPa (right)

These results show that there is a swashplate angle limit around 5 degrees where the pump efficiency dramatically decreases at angles below this. This is because at low swashplate angles the displacement of the pump is small, and the pump subsequently must be driven at high speeds to produce the desired flowrate. At high speeds, the viscous losses begin to dramatically impact the operational efficiency. A reduction in the piston diameter would accomplish the same task as reducing the swashplate angle. Referring to equation (5) and (6), it is shown that a piston reduction would decrease the torque and decrease the flowrate per revolution of the pump. As with the swashplate angle decrease, a piston diameter decrease would require the pump to be driven at a higher speed to produce a certain flowrate. A similar trend occurs with viscous losses beginning to dominate as smaller and smaller piston diameters are used. This trend would likely be seen with all types of pumps, regardless of geometry, due to the fact as the pump displacement per revolution is decreased to reduce torque requirements, the pump must be driven at higher speeds, resulting in increased viscous losses.

The swashplate angle of a small axial-piston pump can be reduced to around 5 degrees to better match the speed-torque characteristics of an electric motor, but it is necessary to determine what range of torques are required by the electric motor for various operating pressures.

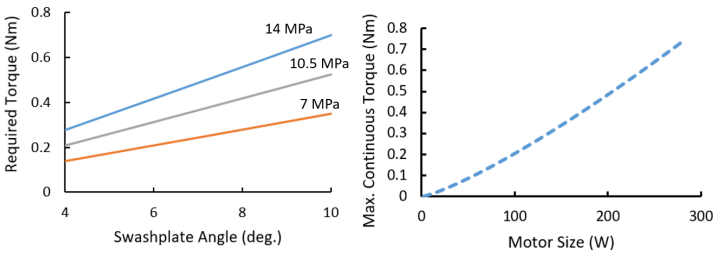

Figure 10. Required motor torque to drive pump (left), maximum continuous motor torque (right)

Figure 10 shows that for a small axial-piston pump, with 3 pistons, 7 mm in diameter, and swashplate angles in the range of 5-8 degrees, the required torques for producing up to 14 MPa pressures are 0.2-0.4 Nm, which requires motors in the range of 150-300 W. Therefore, a gearbox could be eliminated and the electric motor could be directly coupled to the pump, thus eliminating both the added weight of the gearbox itself as well as the added weight of the battery due to the inefficiencies of the gearbox.

Another aspect to consider before eliminating the gearbox is that adding a gearbox can potentially allow for a motor to operate more efficiently, which would reduce the battery weight. Figure 11 shows a case that uses a fixed 150 W size motor driving a fixed 0.17 cc/rev axial-piston pump for a 2 hour runtime at 10 cc/sec. The overall system weight was calculated for various gear reduction ratios applied to the motor-pump connection for pressures of 5 and 15 MPa.

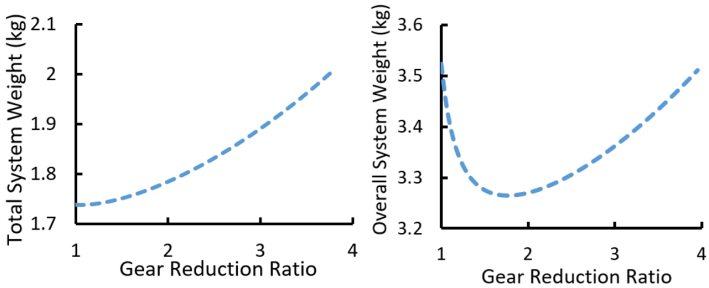

Figure 11. Gear reduction exploration, 5 MPa (left), 15 MPa (right)

For lower pressures, adding a gear reduction does not lower the overall system weight. However, as shown in Figure 11, at higher pressures a gear reduction ratio allows the fixed motor to operate at a higher efficiency, thus resulting in a lower battery weight and a lower overall system weight.

Adding a gearbox was considered for 9 different operating pressures and flowrates. The weight reductions, shown in Figure 12, are equivalent to the amount of battery weight saved due to the optimized gear reduction allowing the motor to operate more efficiently.

	5 cc/sec	10 cc/sec	15 cc/sec
5 MPa	4 g	1 g	0 g
10 MPa	46 g	36 g	31 g
15 MPa	219 g	259 g	354 g

Figure 12. Optimized gearbox battery weight savings, assuming ideal gearbox

Figure 12 shows that only the high pressure, 15 MPa cases benefited from the addition of a gear reduction to allow the motor to operate more efficiently, thus lowering the battery weight. However, this analysis assumed did not consider the weight of the gearbox itself or the inefficiencies that a gearbox would add, which would result in additional battery weight. A small gearbox may be around 150 g itself. For the three 15 MPa cases, if the gearbox operated at an 80% efficiency, it would add 307, 617, and 968 g of battery weight to the 5, 10, and 15 cc/sec cases, thus outweighing the potential battery savings due to the increase in motor efficiency. This demonstrates that a gearbox will ultimately add additional weight to the system and should be avoided. To directly drive the pump with an electric motor, the pump needs have sufficiently low displacements. For motors in the 100-300 W range, the displacement of the pump must be around 0.2 cc/rev or lower to allow pressures up to 14 MPa to be generated. The elimination of the gearbox in this manner will allow for minimization of the overall system weight.

Motor Cooling

A method to reduce system weight could be to use active cooling systems to allow the use of a smaller, lighter motor. There are several tradeoffs that must be considered. As demonstrated by the motor sizing exploration, although a smaller motor is lighter, it is often less efficient than larger motors, thus resulting in more battery weight. This tradeoff must be explored for various operating conditions to assess the potential weight savings. Figure 13 shows the motor size that results in a minimal system weight for various system runtimes. This was done for the same conditions as the study shown in Figure 8, where a fixed 0.17 cc/rev pump was used and operation conditions of 5 MPa and 5 cc/sec were specified. This study demonstrated that the motor size required to produce a minimum system weight for the given conditions was 62 W and 100 W for runtimes of 0.5 and 8 hours. Figure 13 shows the motor size that results in a minimum system weight for a range of desired run times, with all other setup conditions held constant.

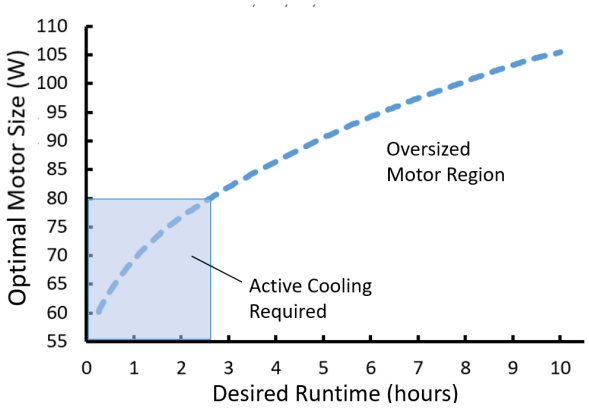

Figure 13. Optimal motor size selection is dependent on runtime, weight of active cooling systems not considered

Figure 13 shows that as the desired runtime is increase, the motor size that results in a minimum system weight also increases. Again, this is because at longer runtimes, the battery weight dominates overall system weight, so using a heavier, more efficient motor is optimal for minimizing system weight. Using the motor model, it was determined that the minimum possible motor size that could drive the pump at continuous conditions of 5 MPa and 5 cc/sec was 81 W to ensure overheating did not occur. This means that for the runtimes under 2.5 hours, where the optimally-sized motor is below 81 W, active cooling would be required to allow the motor to run without overheating. For designed runtimes above 2.5 hours, active cooling would not be required, and oversized motors would produce lower overall system weights.

For active cooling it is useful to determine what the approximate weight savings would be if a cooling system was implemented to allow undersized motors to operate. Figure 14 shows the case for a 0.5 hour runtime, showing the overall system weight for a range of motor sizes. The 46 g difference is the total system weight difference between using active cooling to be able to use the weight-optimum, undersized 62 W motor versus using the minimum 81 W motor without cooling.

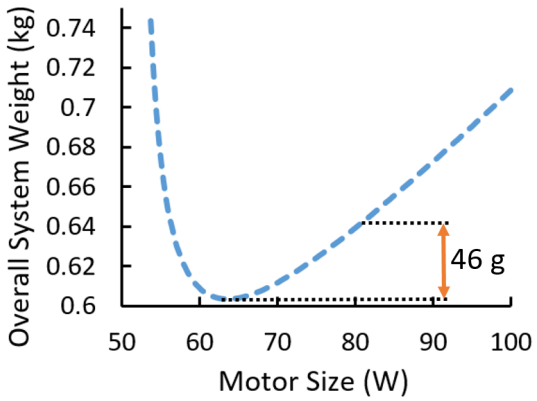

Figure 14. 0.5 hr. runtime, system weight difference between using actively-cooled 62 W motor vs. non-cooled 81 W motor

This 46 g savings, however, does not consider the weight added by the cooling system, which would likely be more than 46 g. Additionally, several different operating pressures, flowrates, and runtimes were investigated to determine the potential weight savings of using undersized motors with active cooling systems. These cases resulted in savings in the range of 40-70 g. A practical cooling system might include a fan as well as additional battery weight needed to power the fan. Although the exact weight and energy consumption requirements for an active cooling system for the motors below 81 W has not been quantified, it is likely that motors 81 W and larger, which do not require active cooling would be the best choice, as the cooling system weight would likely outweigh the weight saved by using a lighter, undersized motor.

Another area where a cooling system might potentially reduce overall weight comes from the resistivity of copper being temperature dependent. As the motor is cooled, the resistivity of the copper windings is reduced, making the electric motor more efficient, thus resulting in a lower battery weight. Figure 15 demonstrates the effect of actively cooling an 80 W motor driving a 0.17 cc/rev pump at 5 MPa and various flowrates.

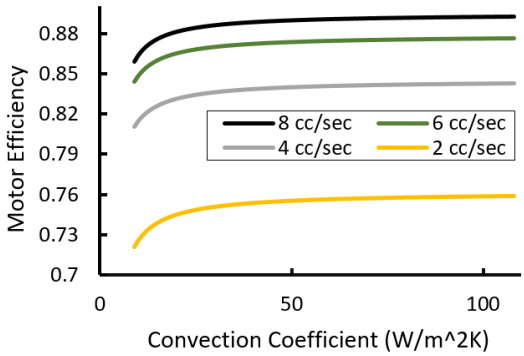

Figure 15. Copper winding losses, temperature dependence

The results show that the temperature difference of the windings due to using active cooling does not have a significant impact on the overall efficiency of the motor. A maximum increase in efficiency of about 3% was observed, which is not sufficient to justify adding in an active cooling system. This shows cooling systems generally do not help reduce overall system weight. However, in real-world applications of such power supplies, cooling systems may still be of potential use to ensure that the motor does not overheat in the case of variations in natural convection cooling conditions.

Total model

A combined system model was used to aid in the design of a complete minimal-weight system. The inputs to the model were desired pressure, flowrate, and runtime. The program was designed to iterate through several combinations of motor size, pump size, and pump swashplate angle. The resulting output was the motor size, pump size, and swashplate angle that resulted in the lowest overall system weight. Figure 16 shows an output from the program with desired 10 MPa pressure, 10 cc/sec flowrate, 2 hour runtime, and a 150 W motor.

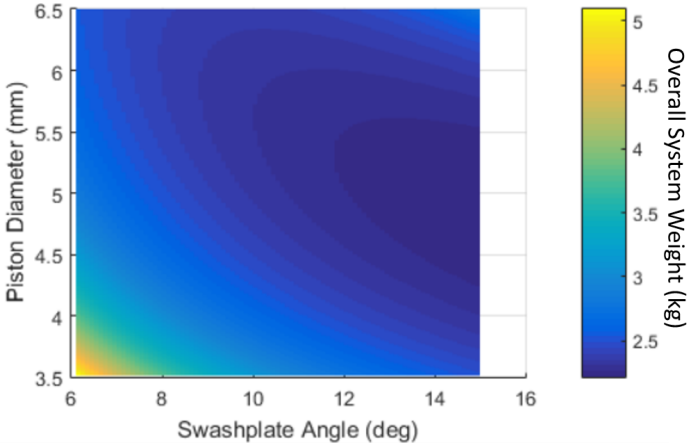

Figure 16. Weight optimization using fixed 150 W motor, variable pump, and desired 10 cc/sec, 10 MPa, 2 hr runtime

The results are a pump size with three pistons, 4 mm in diameter, a 19 º swashplate angle, and 0.11 cc/rev displacement, a motor size of 93 W, and overall system weight of 2.01 kg. As shown by Figure 16, near the lower left corner of the plot, the pump displacement is low, with both small pistons as well as low swashplate angles. As shown earlier, as the displacement of the pump is reduced to small values, viscous losses become large, resulting in high systems weights. This combined system model could be used in the design of a range of desired flowrates, pressures, and runtimes defined by the user.

While the total system model outputs a combination of pump and motor parameters that results in a minimal system weight, Figure 16 shows that there is a range of pump parameters close to the optimal solution that results in a system weight very close to the optimal design. Therefore, the combined system model could be used to either design a fully customized, minimal-weight system or it could be used to aid in the selection of commercially available components that are close to the optimal components determined by the model.

DISCUSSION

The analyses in this study were completed for steady-state operation. Future work will include expanding this model to analyze pseudo-steady-state systems, where multiple steady-state conditions could be applied to each separate analysis. Dynamic motor and pump operation will also be considered.

This analysis has not considered variabilities in construction techniques of an actual power supply. For example, if the electric motor is enclosed in a plastic case, it could change the cooling of the motor. Although it was shown that active cooling does not help reduce overall system weight, active cooling may still be necessary to ensure the motor does not overheat due to unforeseen reductions in normal free convection.

The motor selection, gearbox exploration, and cooling system analyses produced results that suggested using larger electric motors over smaller ones. Larger motors often operate

more efficiently, do not overheat as easily, and can produce higher torques to eliminate the need for a gearbox. Therefore, in addition to the four design guidelines developed, a more general guideline is that when designing such power supplies, it is better to use larger motors than calculated. The models developed contain assumptions and simplifications. Therefore, if the model is being used to select commercially available motors, err on the side of selecting larger motors. Future work will be done to test basic set-ups of battery-motor-pump configurations to further validate the design guidelines and principles.

ACKNOWLEDGMENTS

Funding provided by the National Institute of Health (NIH), grant number 1R21EB019390.

REFERENCES

1] Akers, A., Gassman, M., and Smith, R., Hydraulic Power System Analysis. Taylor & Francis, 2006.

[2] Durfee, W, and Sun, Z., Fluid Power System Dynamics. Center for Compact and Efficient Fluid Power, 2009.

[3] Hunt, T.M., The Hydraulic Handbook. Elsevier, 1996.

[4] Gilbertson, M., Beekman, D., Mohanty, B., Hashemi, S., Lee, S., Van de Ven, J. D., & Kowalewski, T. M. (2016, October). Force Analysis and Modelling of Soft Actuators for Catheter Robots. In *ASME 2016 Dynamic Systems and Control Conference* (pp. V002T25A005-V002T25A005). American Society of Mechanical Engineers.of Physical Medicine & Rehabilitation, **71**(2), pp. 112-115.

[5] Kopp, Carlo. "Exoskeletons for warriors of the future." *Defence Today* 9.2 (2011): 38-40.

[6] National Research Council. 2004. *Meeting the Energy Needs of Future Warriors*. Washington, DC: The National Academies Press. doi:https://doi.org/10.17226/11065.

[7] Neubauer, B., Nath, J., and Durfee, W., 2014. "Design of a portable hydraulic ankle-foot orthosis". In *Engineering in Medicine and Biology Society* (EMBC), 2014 36th Annual International Conference of the IEEE. IEEE, 2014, pp. 1182–1185.

[8] Toliyat, Hamid A., and Gerald B. Kliman, eds. *Handbook of electric motors*. Vol. 120. CRC press, 2004

[9] Yedamale, P., 2003. Brushless DC (BLDC) motor fundamentals. *Microchip Technology Inc*, *20*, pp.3-15.

[10] Wilson, W. E., 1950. Positive-displacement pumps and fluid motors. Pitman, London.

[11] Jeong, H., 2007. "A novel performance model given by the physical dimensions of hydraulic axial piston motors: model derivation". Journal of Mechanical Science and Technology, 21(1), pp. 83–97.

[12] Jicheng, Xia, 2015, "Modeling and Analysis of Small-Scale Hydraulic Systems" PhD. Thesis, University of Minnesota, Minneapolis, MN

[13] Xia, J., & Durfee, W. K., 2014. Experimentally validated Models of O-ring seals for tiny hydraulic cylinders. In *ASME/BATH 2014 Symposium on Fluid Power and Motion Control, FPMC 2014* Web Portal ASME (American Society Of Mechanical Engineers). DOI: 10.1115/FPMC2014-7825

[14] Hashemi, S., & Durfee, W., 2017. Low-Friction, Long-Stroke Rolling Diaphragm Cylinder for Passive Hydraulic Rehabilitation Robots. *In press, ASME Journal of Medical Devices*

[15] Tong, Wei. *Mechanical design of electric motors*. CRC press, 2014.